S & M 3505

Development of Time-of-flight Measurement System for Carrier Transport Characterization of TlBr Semiconductor Detectors

Yusuke Sugai,[1*] Kenichi Watanabe,[1] Sota Hasegawa,[1]
Keitaro Hitomi,[2] and Mitsuhiro Nogami[2]

[1]Department of Applied Quantum Physics and Nuclear Engineering, Kyushu University,
744 Motooka, Nishi-ku, Fukuoka 819-0395, Japan
[2]Department of Quantum Science and Energy Engineering, Tohoku University,
Aoba, Aramaki, Aoba-ku, Sendai 980-8579, Japan

(Received September 4, 2023; accepted December 4, 2023)

Keywords: TlBr semiconductor detector, time of flight, mobility, mobility–lifetime products

Because thallium bromide (TlBr) semiconductor detectors with a wide bandgap show high detection efficiency and energy resolution, room-temperature gamma-ray spectrometers based on such detectors have been developed. In this study, we developed a system for evaluating the carrier transport properties in a TlBr detector, such as the mobility and the mobility–lifetime product ($\mu\tau$ product), in which the time-of-flight method is applied to charge carriers generated by a pulsed laser. In the developed system, the recombination effect and internal electric field distortion were experimentally confirmed to be negligible under the experimental conditions in this study. We determined the electron mobility and $\mu\tau$ product in the TlBr detector to be 25.3 cm^2/Vs and 1.3×10^{-3} cm^2/V, respectively. Because the laser spot diameter is less than 0.5 mm, the constructed measurement system allows the evaluation of the mobility and $\mu\tau$ product at a point on the crystal. It is also possible to evaluate the 2D distribution of the mobility and $\mu\tau$ product by scanning the laser irradiation position.

1. Introduction

Thallium bromide (TlBr) has potential use as a next-generation gamma-ray spectrometer.(1–11) TlBr has a wide bandgap energy of 2.68 eV, which would enable the room-temperature operation of such a spectrometer. It is also composed of elements with high atomic numbers (Tl = 81, Br = 35) and has a high density (7.56 g/cm^3). Therefore, high detection efficiency can be expected. Recent improvements in the purification process of TlBr using zone melting methods have led to higher mobility–lifetime products ($\mu\tau$ products) of electrons and holes.(11) Consequently, some recent studies have achieved a high energy resolution of about 1% for 662 keV gamma rays.(9)

*Corresponding author: e-mail: sugai.yusuke.031@s.kyushu-u.ac.jp
https://doi.org/10.18494/SAM4631

ISSN 0914-4935 © MYU K.K.
https://myukk.org/

The next task in the development of TlBr detectors is to establish a reliable procedure for fabricating large-volume and high-quality detectors. The uniformity of the crystal quality and charge transport property is important for large detectors with high performance. Thus far, we have evaluated the crystal quality of TlBr using neutron Bragg dip imaging and electron beam backscatter diffraction (EBSD).[12,13] However, there is no knowledge of the correlation between the crystal quality and the charge transport properties. To clarify this correlation, we have developed a time-of-flight (TOF) measurement system that can evaluate the 2D distribution of charge transport properties within crystals. The system is based on the TOF of charge carriers generated near the surface of a crystal by pulsed and focused laser irradiation. We can evaluate the carrier velocity or mobility using this method.[14] The $\mu\tau$ product of the carriers in this system, which can be derived from the applied electric field dependence of the charge collection efficiency, can also be evaluated. In addition, we can obtain the 2D distribution of these carrier transport properties by scanning the laser spot on the detector surface. In this study, we construct the measurement system and demonstrate carrier velocity and charge collection efficiency measurements. Through these experiments, we confirm the validity of the constructed system.

2. Materials and Methods

2.1 Sample preparation

Before the crystal growth procedure, TlBr was processed by the zone purification method.[11] Purification was carried out more than 100 times with a heater temperature of about 500 °C and a passing speed of 50 mm/h. Then, crystals were grown by the traveling molten zone method with a heater speed of 1 mm/h. The grown TlBr crystal was cut to a size of $5 \times 5 \times 2.36$ mm^3 with a diamond wire saw (model 3500, Well) and both 5×5 mm^2 surfaces were polished. Gold electrodes were formed on these two faces using a vacuum evaporation system (SVC-700TMSG, SANYU). The thickness of the electrodes was approximately 100 nm.

2.2 TOF measurement system

Figure 1(a) shows a conceptual drawing of the TOF measurement system. A negative voltage, which was changed from −100 to −500 V for each measurement, was applied to the cathode electrode by a high-voltage power supply (DT5470N, CAEN). A pulsed laser (NPL41C, Thorlabs) with a wavelength of 405 nm was used as the laser source. The laser transmittance of a 100-nm-thick gold electrode was roughly estimated to be 4×10^{-4} from the relationship between the irradiated laser energy and the induced charge. The pulse width was varied, with a maximum pulse width of 128 ns. The pulse energy was changed by varying the pulse width. The maximum pulse energy was 128 nJ. The laser beam was focused with a lens (LA1134-A, Thorlabs) to the cathode side of the detector. The focused spot diameter was less than 0.5 mm. The laser-irradiated TlBr detector is shown in Fig. 1(b). Part of the laser light passed through the cathode electrode and was absorbed within a few tens of nanometers from the crystal surface. As a result, a large number of electron–hole pairs were generated immediately below the cathode.

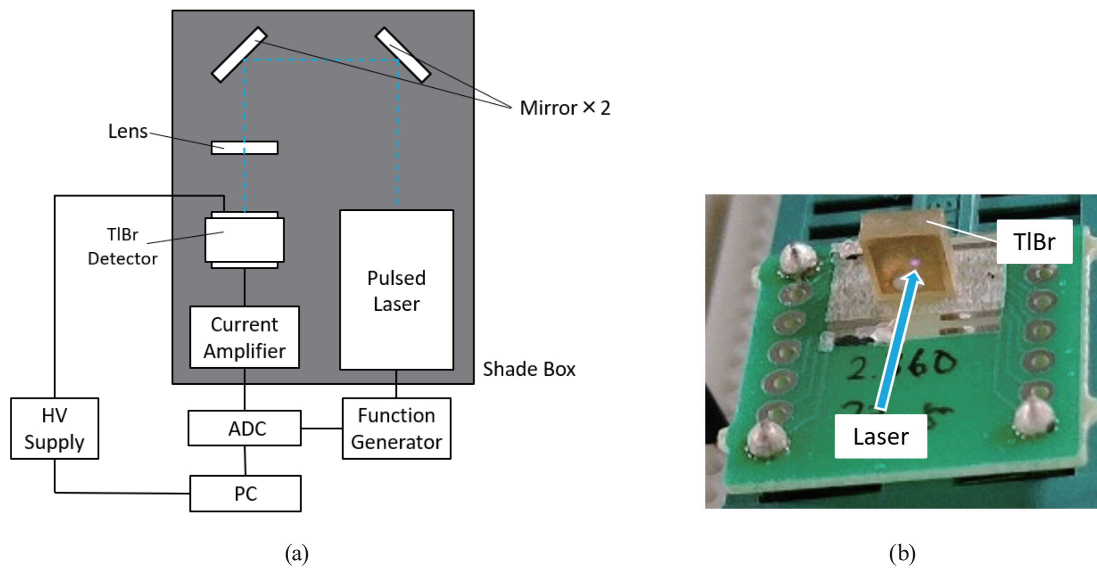

(a) (b)

Fig. 1. (Color online) (a) Experimental setup of the TOF measurement system used to characterize the carrier transport properties of TlBr detectors. (b) Photograph of a TlBr detector irradiated with focused laser pulses.

Because of the applied electric field, the generated holes immediately reached the cathode, whereas the electrons moved to the anode side. The induced signal current was amplified by a current amplifier (TIA60, Thorlabs) and digitized by an analog-to-digital converter (ADC) (model 1820, CLEAR-PULSE). Data were collected and analyzed on a PC. The pulsed laser and ADC were synchronized with 100 Hz trigger pulses. The entire experimental setup was enclosed within a shade box to shield the system from ambient light.

3. Results and Discussion

Figure 2 shows the signal waveforms obtained when irradiating the detector by laser pulses with an energy of 128 nJ. The TOF and induced current were changed by varying the applied voltage, indicating that the velocity of the charge carriers depends on the applied electric field. The carrier migration velocity was derived from the TOF.

The energy of the pulsed laser was rather high compared with that of typical gamma-ray photons, for example, 662 keV from Cs-137. Assuming a transmittance of 1% for the pulsed laser through the thin gold electrode, the energy deposited onto the crystal was 1.28 nJ or 8 GeV for the maximum laser energy of 128 nJ. Under these conditions, a large number of electron–hole pairs were generated, which might lead to carrier recombination and distort the internal electric field. Therefore, we first investigated the effect of the pulsed laser energy on the signal waveforms. The signal waveforms were compared for various pulsed laser energies at different applied voltages. Figure 3 shows the current signal waveforms obtained by irradiating the TlBr detector with pulses of various energies. Each waveform was averaged over 1000 laser pulses. The current signal waveforms were normalized by the pulse energy. The waveforms obtained at

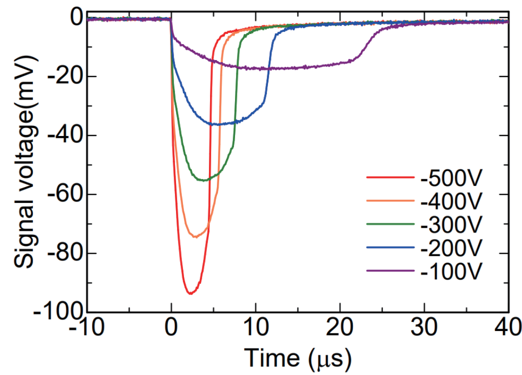

Fig. 2. (Color online) Signal waveforms induced by transport of electrons generated by pulsed laser irradiation. Each waveform was averaged over 1000 laser pulses.

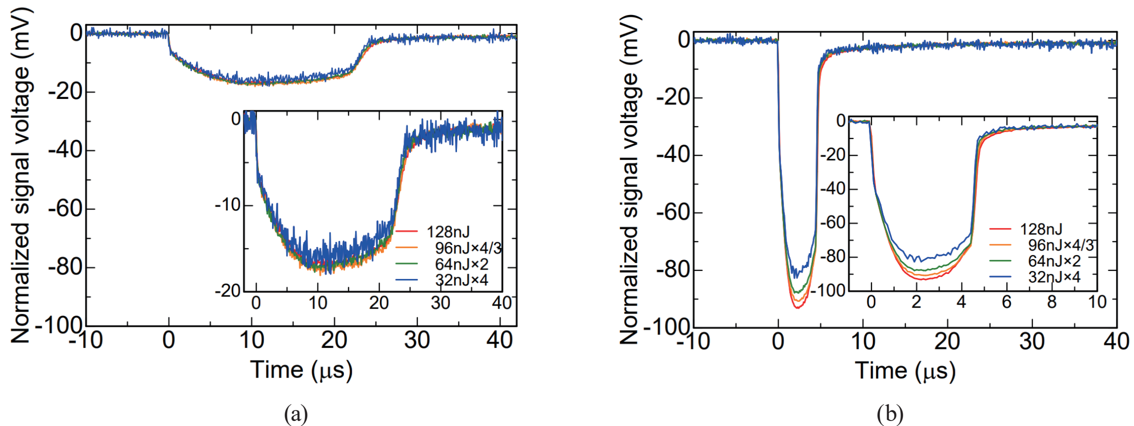

Fig. 3. (Color online) Signal waveforms obtained by irradiating the TlBr detector with pulses of various energies. Voltages of (a) −100 and (b) −500 V were applied to the cathode.

different applied voltages are also presented. Because the shape of the signal waveforms is independent of the pulse energy, we conclude that the effects of the recombination and distortion of the internal electric field are negligible under the present experimental conditions.

The carrier migration velocity was derived from the thickness of the crystal, which is the distance of carrier migration, and the carrier migration time, or TOF. The carrier migration time was determined from the pulse width of the induced current signal as shown in Fig. 3. The electric field intensity was assumed to be constant inside the crystal because a planar detector configuration was applied. Figure 4 shows the dependence of the electron migration velocity on the applied electric field. The carrier velocity was demonstrated to be proportional to the electric field. The electron mobility μ_e is defined as the proportionality constant between the carrier velocity and the electric field. μ_e was found to be 25.3 cm^2/Vs. This value is reasonable compared with those in previous studies.[14]

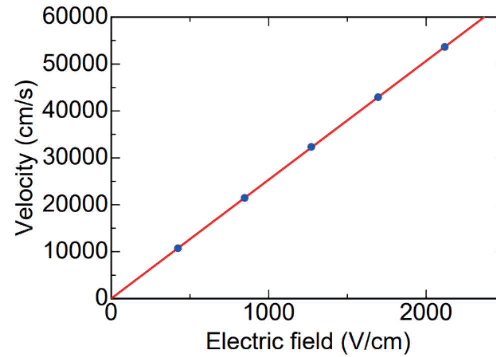

Fig. 4. (Color online) Dependence of the electron velocity in the TlBr detector on the electric field.

The amount of induced charge Q was calculated using the following equation:

$$Q = \int I\,dt = \frac{1}{R}\int V_{sig.}\,dt\,, \tag{1}$$

where R (V/A) is the gain of the transimpedance amplifier and V_{sig} (V) is the signal voltage. The integral value of the current signal pulse corresponds to the total charge induced on the readout electrode. From the dependence of the induced charge Q on the applied voltage, the carrier $\mu\tau$ product can be evaluated using Hecht's equation.(15,16) Q can be expressed as

$$Q = CV\{1 - \exp\left(\frac{L^2}{\mu\tau V}\right)\}\,, \tag{2}$$

where C is a constant, V is the applied voltage, L is the thickness of the TlBr detector, and μ and τ are the electron mobility and lifetime, respectively. Figure 5 shows the dependence of Q on the applied voltage. The $\mu\tau$ product of electrons $(\mu\tau)_e$ was found to be 1.3×10^{-3} cm^2/V by fitting the data to Hecht's equation. This value is also acceptable in consideration of results in previous studies.(11) On the basis of the above measurements, we conclude that the developed measurement system can adequately evaluate the mobility and $\mu\tau$ product of a TlBr semiconductor detector. Because the laser spot diameter is less than 0.5 mm, it is also possible to measure the 2D distribution of the mobility and $\mu\tau$ product by scanning the laser irradiation position on the crystal with a planar detector.

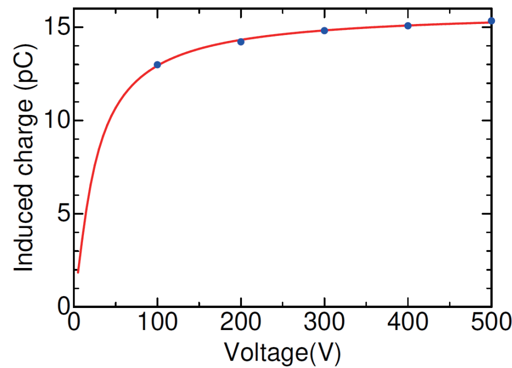

Fig. 5. (Color online) Dependence of Q on the voltage applied to the cathode.

4. Conclusions

We developed a system for evaluating the mobility and μτ product of electrons generated by a pulsed laser, in which the TOF method was applied. The validity of the developed system was investigated through fundamental experiments. Since the production of carriers using a pulsed laser generates a large number of electron–hole pairs, carrier recombination and internal electric field distortion were concerns. Therefore, we experimentally confirmed that these effects were negligible under the present experimental conditions. Under these conditions, the mobility of electrons, μ_e, in the detector used in this study was determined to be 25.3 cm^2/Vs. Using Hecht's equation, the μτ product of electrons $(\mu\tau)_e$ was determined to be 1.3×10^{-3} cm^2/V. These values are reasonable compared with those in previous works. Because the laser spot diameter is less than 0.5 mm, it is also possible to measure the 2D distribution of the mobility and μτ product by scanning the laser irradiation position on the crystal with a planar detector.

As future works, this system will be upgraded for 2D measurements, for which it will be equipped with a two-axis linear stage, and the signal waveforms will be automatically acquired. Then, we will compare the 2D distribution of the carrier transport properties with the distribution of the crystal orientation evaluated using neutron diffraction imaging and EBSD. Finally, we will investigate the correlation between the crystal quality and the carrier transport properties.

Acknowledgments

This work was partially supported by JSPS KAKENHI Grant Number JP 22H02008. It was also partially supported by the Cooperative Research Project of Research Institute of Electronics, Shizuoka University.

References

1 K. Hitomi, T. Murayama, T. Shoji, T. Suehiro, and Y. Hiratate: Nucl. Instrum. Methods Phys. Res. A **428** (1999) 372.
2 K. Hitomi, O. Muroi, T. Shoji, T. Suehiro, and Y. Hiratate: Nucl. Instrum. Methods Phys. Res. A **436** (1999) 160.
3 T. Onodera, K. Hitomi, T. Shoji, and Y. Hiratate: Nucl. Instrum. Methods Phys. Res. A **525** (2004) 199.
4 K. Hitomi, T. Onodera, T. Shoji, and Z. He: Nucl. Instrum. Methods Phys. Res. A **578** (2007) 235.
5 K. Hitomi, T. Shoji, and Y. Niizeki: Nucl. Instrum. Methods Phys. Res. A **585** (2008) 102.
6 K. Hitomi, Y. Kikuchi, T. Shoji, and K. Ishii: Nucl. Instrum. Methods Phys. Res. A **607** (2009) 112.
7 B. Donmez, Z. He, H. Kim, L. J. Cirignano, and K. S. Shah: Nucl. Instrum. Methods Phys. Res. A **623** (2010) 1024.
8 K. Hitomi, T. Shoji, and K. Ishii: J. Cryst. Growth **379** (2013) 93.
9 K. Hitomi, T. Tada, T. Onodera, S-Y. Kim, Y. Xu, T. Shoji, and K. Ishii: IEEE Trans. Nucl. Sci. **60** (2013) 1156.
10 K. Hitomi, T. Onodera, S-Y. Kim, T. Shoji, and K. Ishii: Nucl. Instrum. Methods Phys. Res. A **747** (2014) 7.
11 K. Hitomi, T. Onodera, and T. Shoji: Nucl. Instrum. Methods Phys. Res. A **579** (2007) 153.
12 K. Watanabe, K. Matsumoto, A. Uritani, K. Hitomi, M. Nogami, and W. Kockelmann: Sens. Mater. **32** (2020) 1435.
13 B. L. Adamus, S. I. Wright, and K. Kunze: Metall. Trans. A **24** (1993) 819.
14 K. Suzuki, M, Shorohov, T. Sawada, and S. Seto: IEEE Trans. Nucl. Sci. **62** (2015) 433.
15 K. Hecht: Z Phys. **77** (1932) 235.
16 Z. He, G.F. Knoll, and D. K. Wehe: J. Appl. Phys. **84** (1998) 5566.